Feasibility of ^{11}C-Acetate PET/CT for Imaging of Fatty Acid Synthesis in the Atherosclerotic Vessel Wall

Thorsten Derlin[1], Christian R. Habermann[2], Zsolt Lengyel[3], Jasmin D. Busch[2], Christian Wisotzki[1], Janos Mester[1], and László Pávics[4]

[1]Department of Nuclear Medicine, University Medical Center Hamburg-Eppendorf, Hamburg-Eppendorf, Germany; [2]Department of Diagnostic and Interventional Radiology, University Medical Center Hamburg-Eppendorf, Hamburg, Germany; [3]Pozitron Ltd., Budapest, Hungary; and [4]Department of Nuclear Medicine, University of Szeged, Szeged, Hungary

Fatty acids are a common constituent of atherosclerotic plaque and may be synthesized in the plaque itself. Fatty acid synthesis requires acetyl-coenzyme-A (CoA) as a main substrate, which is produced from acetate. Currently, ^{11}C-acetate PET/CT is used for the evaluation of malignancies. There are no data concerning its potential for the characterization of atherosclerotic plaque. Therefore, the purpose of the present study was to examine the prevalence, distribution, and topographic relationship of arterial ^{11}C-acetate uptake and vascular calcification in major arteries. **Methods:** Thirty-six patients were examined by whole-body ^{11}C-acetate PET/CT. Tracer uptake in various arterial segments was analyzed both qualitatively and semiquantitatively by measuring the blood-pool–corrected standardized uptake value (target-to-background ratio). CT images were used to measure calcified plaque burden. **Results:** ^{11}C-acetate uptake was observed at 220 sites in 32 (88.8%) of the 36 study patients, and mean target-to-background ratio was 2.5 ± 1.0. Calcified atherosclerotic lesions were observed at 483 sites in 30 (83.3%) patients. Sixty-four (29.1%) of the 220 lesions with marked ^{11}C-acetate uptake were colocalized with arterial calcification. However, only 13.3% of all arterial calcification sites demonstrated increased radiotracer accumulation. **Conclusion:** Our data indicate the feasibility of using ^{11}C-acetate PET/CT for imaging of fatty acid synthesis in the atherosclerotic vessel wall. This study provides a rationale to incorporating ^{11}C-acetate PET into further preclinical and clinical studies to obtain new insights into fatty acid synthesis in atherosclerotic lesions and to evaluate whether it may be used to monitor pharmacologic intervention with fatty acid synthase inhibitors.

Key Words: ^{11}C-acetate; atherosclerosis; cardiovascular; fatty acid synthase; calcification; PET/CT

J Nucl Med 2011; 52:1848–1854
DOI: 10.2967/jnumed.111.095869

Atherosclerosis and its atherothrombotic complications remain among the leading causes of morbidity and mortality in the developed world, and their prevalence is likely to increase because of growing obesity rates (*1,2*). The structure, biologic composition, and inflammatory state of atherosclerotic plaque are the major determinants of the acute risk of atherothrombotic events, rather than the degree of luminal stenosis (*3,4*). Vulnerable atheroma have been shown to contain a large lipid core, a thin fibrous cap, fewer smooth muscle cells than stable plaque, and a preponderance of lipid-filled macrophages (*5–7*). In particular, several studies have shown that structurally vulnerable, rupture-prone plaque may contain a large, fatty acid–rich lipid core greater than 40% of the total lesion area (*8,9*). Therefore, further morphofunctional characterization of atherosclerotic plaque is needed to understand the different pathophysiologic aspects of formation and progression of plaque, identify vulnerable atherosclerotic lesions that are particularly prone to rupture, and eventually guide therapeutic interventions.

In recent years, the potential of molecular imaging technologies such as PET/CT to further characterize pathophysiologic processes in atherosclerotic lesions has been extensively studied (*10*). Various both experimental and clinical studies have shown the reliability of ^{18}F-FDG PET/CT in imaging and quantifying macrophage-mediated inflammation in plaque (*11–13*). Other studies have targeted different pathophysiologic aspects of plaque including cell membrane proliferation or active mineral deposition using ^{11}C-choline or ^{18}F-sodium fluoride, respectively (*14,15*).

Lipids are a major constituent of atherosclerotic lesions and play a key role in the development and progression of plaque (*3,5*). Apart from cholesterol, which is mainly accumulated in the form of cholesteryl esters, phospholipids and triglycerides are also abundantly found in plaque, all of which contain fatty acids (*16*). There is strong evidence these fatty acids in atheromatous plaque are not only derived from diet but also from de novo fatty acid synthesis within arterial wall lesions, because several studies have demonstrated the ability of the arterial vasculature for de novo lipid synthesis (*17,18*). Fatty acid synthesis is an energy-consuming process creating fatty acids through action of the multifunctional enzyme fatty acid synthase (FAS), which requires acetyl-coenzyme-A (CoA) produced from acetate as substrate (*19*).

Received Jul. 21, 2011; revision accepted Sep. 26, 2011.
For correspondence or reprints contact: Thorsten Derlin, University Hospital Hamburg-Eppendorf, Department of Nuclear Medicine, Martinistrasse 52, 20246 Hamburg-Eppendorf, Germany.
E-mail: t.derlin@uke.uni-hamburg.de
Published online Nov. 7, 2011.

These fatty acids are crucial for the intralesional differentiation of monocytes into macrophages with phagocytotic capacity, ultimately forming foam cells (*20,21*). Additionally, fatty acids are involved in the regulation of lipid homeostasis and macrophage inflammatory responses (*3*). Thus, there are dynamic and complex interactions between macrophages and lipids such as fatty acids in atherosclerotic plaque. Consequently, inhibition of macrophage fatty acid synthesis decreases diet-induced atherosclerosis in mice (*22*). In short, intraplaque fatty acid synthesis contributes to plaque growth and is essential for macrophage-mediated inflammation and therefore functional stability, and massive fatty acid accumulation also decreases the structural stability of the plaque. Therefore, ^{11}C-acetate PET/CT may have the potential to provide information about distinct pathophysiologic aspects of key plaque-related variables such as development, progression, and stability of plaque.

^{11}C-acetate PET/CT has become an established and well-studied imaging procedure for both the evaluation of malignant tumors and myocardial oxidative metabolism (*23–25*). However, to our knowledge, there are no published data on the value of ^{11}C-acetate PET for imaging of vessel wall alterations. Therefore, the purpose of the present study was to analyze the prevalence, distribution, and topographic relationship of arterial lesions with increased ^{11}C-acetate accumulation as determined by PET relative to arterial calcification as assessed by CT in a cohort of asymptomatic patients.

MATERIALS AND METHODS

Study Population

Thirty-six patients (5 women, 31 men; mean age ± SD, 60.4 ± 10.6 y; age range, 29.5–71.5 y) who had been referred for an ^{11}C-acetate PET/CT scan from March 2007 to May 2011 due to an oncologic indication were enrolled in our study. Patients with a history of vasculitis, systemic rheumatic disease, or chemotherapy in the preceding 4 wk were excluded from the analysis. Cardiovascular risk factors including age, sex, hypertension, body mass index, and a history of prior cardiovascular events (defined as myocardial infarction, stroke, or revascularization procedure) were documented from charts. Treatment with statins and the use of other cardiac medication (i.e., β-blockers, angiotensin-converting enzyme inhibitors, and angiotensin II receptor antagonists) were recorded, because statins may affect plaque physiology (*26*). The study protocol had been approved by the local Institutional Review Board and complied with the Declaration of Helsinki. All subjects had given written informed consent.

PET/CT Protocol and Image Reconstruction

All PET/CT examinations were performed using a commercially available PET/CT scanner (Biograph TruePoint HD 6; Siemens Medical Solutions). All patients had fasted for at least 4 h before intravenous injection of 500 ± 50 MBq of ^{11}C-acetate. Whole-body PET/CT data were acquired beginning at about 15 min after tracer injection with an axial field of view of 21 cm and 3 min per bed position. Images were iteratively reconstructed into a 168 × 168 matrix. According to the standardized protocol used at our institution, the CT scans were performed using the following imaging parameters: field of view, 70 cm; matrix, 512 × 512; section thickness, 5 mm; collimation, 6 × 3 mm; pitch, 1.5; rotation speed, 0.6 s; tube voltage, 130 kV; and tube current–time product, 70–90 mAs. Intravenous contrast agent was not administered. The resulting PET and CT scans were coregistered using the standard software tool of the system software.

Image Analysis

PET, CT, and PET/CT fusion images were evaluated both visually and semiquantitatively using a dedicated PET/CT workstation (Extended Brilliance Workstation EBW; Philips). The analysis was performed on the basis of lesions and arterial segments. For the segment-based analysis, the major arteries were subdivided as follows: right and left common carotid arteries, thoracic aorta, abdominal aorta, and right and left iliac arteries.

Radiotracer Uptake. PET images were evaluated for the presence of focal radiotracer uptake in arterial walls. The localization of these areas in relation to the vascular wall and to calcifications was determined in PET/CT fusion images. Semiquantitative analysis was performed by obtaining the maximum standardized uptake value (SUV_{max}) and blood-pool SUVs that were the mean from 3 regions interest of fixed size placed in the mid lumen of the vena cava superior. The SUV_{max} of each arterial lesion was divided by the blood-pool SUVs, yielding an arterial target-to-background ratio (TBR), which is reported subsequently (*12*).

Calcified Plaque (CP). CT images were evaluated for the presence of CPs in the wall of the studied arteries, defined as high-density mural areas (attenuation > 130 Hounsfield units). Patients were divided into those with CP and those without discernible CP. Each CP was classified on a scale for grading circumferential extent, as described previously (*15*).

Statistical Analysis

Categoric variables are presented with absolute and relative frequencies. Continuous variables are given as mean ± SD. For between-group comparisons of continuous data, *P* values were calculated from Mann–Whitney *U* rank sum tests. For categoric variables, *P* values were computed from contingency tables using the Fisher exact test. The Spearman coefficient r_s was used for correlation analysis. Statistical significance was established for *P* values of less than 0.05. Statistical analysis was performed using GraphPad Prism 5.0 (GraphPad Software) for Windows (Microsoft).

To test intra- and interrater agreement, assessment of calcification and radiotracer uptake was repeated 4 wk after the initial review by the same reader and by a second reviewer. Cohen κ with 95% confidence interval (CI) was calculated to measure both intra- and interrater agreement.

RESULTS

Study Population

^{11}C-acetate uptake measurements and the evaluation of CP burden were feasible in all patients. The 36 recruited patients (mean age ± SD, 60.4 ± 10.6 y; age range, 29.5–71.5 y) included 5 women and 31 men. All patients were clinically stable and asymptomatic for cardiovascular disease when imaged.

Arterial Wall ^{11}C-Acetate Uptake and CP Burden

Focally increased vascular uptake of ^{11}C-acetate was seen at 220 sites in 32 (88.8%) of the 36 study patients (Table 1). The prevalence of uptake sites was highest in the abdominal aorta, followed by the thoracic aorta and the iliac arteries.

TABLE 1
Prevalence, Distribution, and Intensity of ^{11}C-Acetate Accumulation

Parameter	Right common carotid	Left common carotid	Thoracic aorta	Abdominal aorta	Right iliac arteries	Left iliac arteries	Total
No. of patients with ^{11}C-acetate uptake in artery wall	2 (6)	9 (25)	20 (56)	28 (78)	12 (33)	13 (36)	32 (100)
No. of uptake sites	2 (1)	12 (5)	50 (23)	106 (48)	21 (10)	29 (13)	220 (100)
SUV_{max}							
Mean	1.0 ± 0.6	1.4 ± 1.0	1.4 ± 0.7	1.8 ± 0.8	1.6 ± 0.6	1.3 ± 0.7	1.6 ± 0.8
Range	0.6–1.4	0.2–3.6	0.3–3.5	0.3–4.5	0.2–3.0	0.2–3.0	0.2–4.5
TBR							
Mean	2.3 ± 1.3	2.0 ± 0.6	2.4 ± 0.8	2.8 ± 1.0	2.6 ± 0.9	2.0 ± 0.8	2.5 ± 1.0
Range	1.4–3.2	1.3–3.5	1.1–4.4	1.1–5.5	1.3–4.4	1.0–4.4	1.0–5.5

Values are mean ± SD, and data in parentheses are percentages.

Mean SUV_{max} was 1.6 ± 0.8, and values ranged from 0.2 to 4.5. Mean blood-pool SUV was 0.6 ± 0.4 (range, 0.1 to 2.3). Mean TBR was 2.5 ± 1.0, and values ranged from 1.0 to 5.5. Both SUV_{max} and blood-pool–corrected TBR were highest in the abdominal aorta.

CPs were observed at 483 sites in 30 (83.3%) of the 36 study patients (Table 2). The prevalence of CP was also highest in the abdominal aorta, followed by the thoracic aorta. Mean calcified lesion thickness was 2.8 ± 1.1 (range, 0.6–7.3). Mean calcification score was 1.5 ± 0.7. For 2 (6%) patients, no arterial wall alteration was found by either PET or CT. Compared with the rest of the study population, these patients were found to be significantly younger (30.0 ± 1.4 y vs. 62.2 ± 7.9 y, $P = 0.02$).

Relationship Between ^{11}C-Acetate Uptake and Calcified Atherosclerotic Lesions

When the topographic relationship between arterial ^{11}C-acetate accumulation and calcification sites was analyzed on a per-segment basis, 71 (33%) of the 216 total segments were found to be PET-positive (+) and CT+, 13 (6%) were PET+ and CT-negative (−), 54 (25%) were PET− and CT+, and 78 (36%) were PET− and CT−. On a per-segment basis, the presence of vascular radiotracer uptake was significantly associated with calcified atherosclerotic lesions within the arterial wall of these segments, representing an established marker of atherosclerotic disease ($P < 0.0001$).

On a per-lesion basis, 156 (70.9%) of the 220 total lesions with radiotracer accumulation showed no correspondence of uptake and calcification. For the remaining 64 (29.1%) arterial lesions with increased ^{11}C-acetate uptake, concordant calcification was observed in at least some part of the affected vessel wall alteration. However, only these 64 (13.3%) of the total 483 CPs showed prominent radiotracer accumulation. In CP, no statistically significant correlation was found between TBR and calcified lesion thickness ($r_s = -0.04$, $P = 0.53$). There was a significant inverse correlation between intensity of radiotracer accumulation (TBR) and calcification score ($r_s = -0.18$, $P = 0.02$). Examples of arterial wall ^{11}C-acetate uptake with and without coincident calcification are shown in Figures 1–3.

Relationship Between ^{11}C-Acetate Uptake, CP, and Risk Factors

The prevalence of arterial tracer accumulation was significantly associated with age ($r_s = 0.45$, $P < 0.01$). Male sex was significantly associated with the presence of arterial radiotracer uptake ($r_s = 0.37$, $P = 0.03$). There was a trend toward a higher prevalence of arterial calcification in older patients, without reaching statistical significance ($r_s = 0.28$, $P = 0.09$). Male sex was not significantly associated with the presence of CP ($r_s = 0.04$, $P = 0.84$).

There was no significant correlation between hypertension and arterial tracer uptake ($r_s = 0.14$, $P = 0.41$) or calcification ($r_s = -0.04$, $P = 0.84$). Neither ^{11}C-acetate accumulation ($r_s = 0.06$, $P = 0.73$) nor CP ($r_s = 0.0$, $P = 0.66$) was significantly associated with prior cardiovascular events. Neither the presence of vascular calcification ($r_s = -0.12$, $P = 0.48$) nor arterial tracer uptake ($r_s = -0.29$, $P = 0.09$) demonstrated a significant correlation with body mass index. Additionally, neither the presence of vascular tracer accumulation ($r_s = 0.14$, $P = 0.41$) nor CP ($r_s = 0.18$, $P = 0.29$) correlated significantly with statin therapy. The use of cardiac medication was not significantly associated with tracer uptake ($r_s = 0.17$, $P = 0.31$) or CP ($r_s = 0.03$, $P = 0.86$).

Reproducibility

Interreader Cohen κ was 0.94 (95% CI, 0.90–0.99) for calcification and 0.89 (95% CI, 0.83–0.95) for tracer uptake in arterial segments. Intrareader Cohen κ was 0.95 (95% CI, 0.91–0.99) for calcification and 0.94 (95% CI, 0.89–0.99) for radiotracer accumulation.

TABLE 2
Prevalence, Distribution, and Extent of Calcification in Studied Arterial Walls

Parameter	Right common carotid	Left common carotid	Thoracic aorta	Abdominal aorta	Right iliac arteries	Left iliac arteries	Total
No. of patients with calcification sites	12 (33)	14 (39)	24 (67)	28 (78)	24 (67)	23 (64)	30 (83)
No. of calcification sites	17 (4)	32 (7)	123 (25)	163 (34)	69 (14)	79 (16)	483 (100)
No. of calcification sites per affected segment	1.4 ± 0.5	2.3 ± 1.1	5.1 ± 5.7	5.8 ± 4.3	2.9 ± 2.5	3.4 ± 1.9	3.1 ± 3.4
Calcification score for lesions	1.4 ± 0.7	1.3 ± 0.7	1.3 ± 0.6	1.4 ± 0.7	1.6 ± 0.8	1.7 ± 0.8	1.5 ± 0.7
Calcified lesion thickness (mm)							
Mean	2.5 ± 1.4	2.2 ± 1.0	3.1 ± 1.3	2.5 ± 1.0	3.0 ± 1.1	3.0 ± 1.1	2.8 ± 1.1
Range	0.9–6.4	0.8–5.1	0.9–7.3	0.6–5.7	0.9–7.3	1.0–7.0	0.6–7.3

Values are mean ± SD, and data in parentheses are percentages.

DISCUSSION

To our knowledge, this is the first study that reports on the association of ^{11}C-acetate uptake with arterial wall alterations in large arteries. Our results indicate the feasibility of using ^{11}C-acetate PET for in vivo imaging of FAS activity in arterial wall lesions. Although mainly used for the evaluation of both malignant tumors and myocardial oxidative metabolism to date, our results suggest that ^{11}C-acetate may be able to depict active fatty acid synthesis in the atherosclerotic vessel wall.

^{11}C-acetate uptake was observed in both calcified and noncalcified vessel wall alterations, and the distribution of tracer accumulation was consistent with established atherosclerotic topography—that is, most active lesions were noted in the abdominal and thoracic aorta (*15,27*), as was also true for calcifications representing a well-known marker of atherosclerosis. Furthermore, arterial tracer uptake correlated significantly with established atherogenic risk factors such as age ($P < 0.01$) and male sex ($P = 0.03$). Radiotracer uptake was not significantly associated with other atherogenic risk factors such as hypertension or a history of cardiovascular events in our study, as is possibly explained by the limited statistical power due to the relatively small number of patients included. In contrast, the observed significant correlations become even more compelling, considering that the study population was not large enough to find significant correlations between risk factors and CP, presenting an established

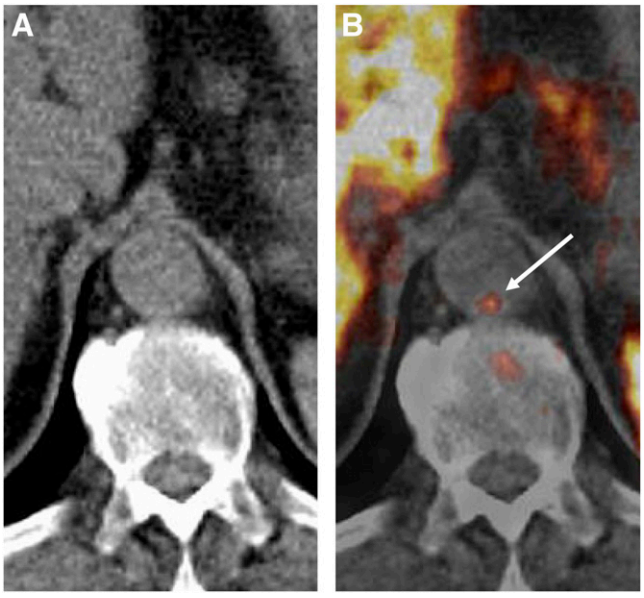

FIGURE 1. Transaxial ^{11}C-acetate PET/CT images of abdominal aorta of 63-y-old man: CT image (A) and coregistered and fused PET/CT image (B). ^{11}C-acetate accumulation in vessel wall alteration was not colocalized with calcification. Arrow = tracer uptake site.

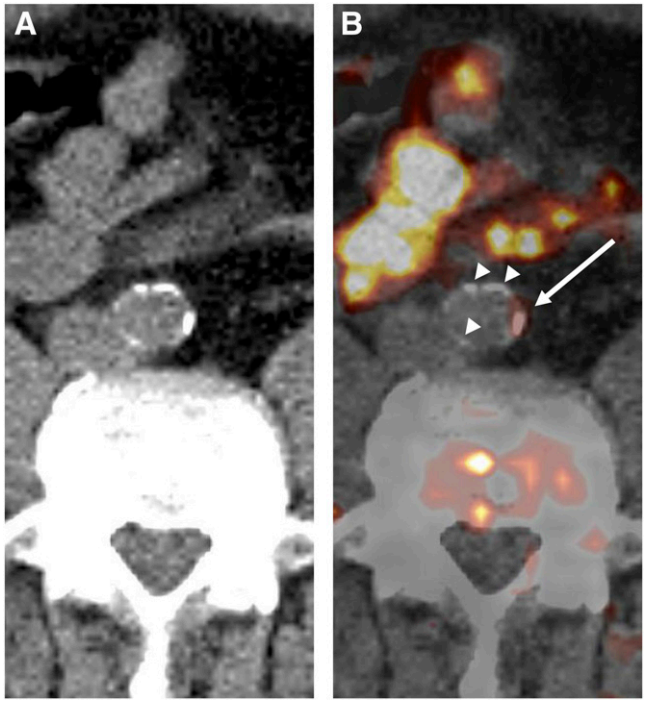

FIGURE 2. Transaxial ^{11}C-acetate PET/CT images of abdominal aorta of 67-y-old man: CT image (A) and coregistered and fused PET/CT image (B). ^{11}C-acetate uptake in vessel wall alteration coincided with calcification. Other CPs of comparable size did not accumulate ^{11}C-acetate. Arrow = tracer uptake site; arrowheads = calcifications.

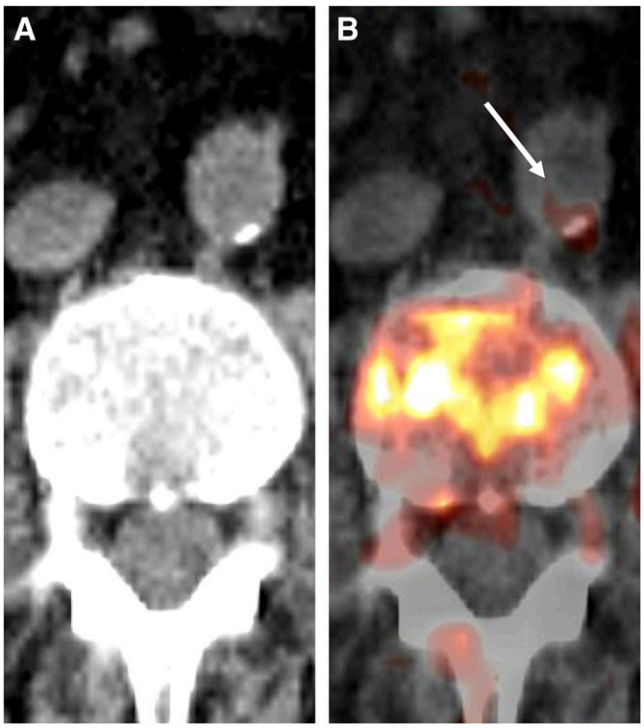

FIGURE 3. Transaxial ^{11}C-acetate PET/CT images of abdominal aorta of 72-y-old man: CT image (A) and coregistered and fused PET/CT image (B). Radiotracer accumulation in vessel wall alteration was mainly colocalized with calcification but expands beyond hyperdense lesion. Arrow = tracer uptake site.

marker of atherosclerosis. Therefore, ^{11}C-acetate uptake demonstrates stronger correlations with at least some determinants of cardiovascular risk than arterial calcification. The use of ^{11}C-acetate as a novel PET tracer for imaging of arterial wall lesions may hold potential to provide information about intralesional fatty acid synthesis in both formation and evolution of atherosclerotic lesions.

With regard to the colocalization of tracer accumulation and calcification sites, the findings of this study add novel observations about ^{11}C-acetate, compared with other tracers used for characterization of atherosclerotic lesions. Various studies reported colocalization in about 2%–14% of sites, using ^{18}F-FDG as a marker of macrophage activity (*27–29*). When ^{18}F-sodium fluoride is used as an indicator of active mineral deposition, uptake has been shown to be coincident with calcification in up to 88% of sites (*15*). In the present study, no colocalization of ^{11}C-acetate accumulation with calcification was observed in 70.9% of lesions with tracer uptake, suggesting that increased fatty acid synthesis is of particular pathophysiologic importance in noncalcified vessel wall alterations, which are usually assumed to represent early stages of disease (*3*). Consequently, no coincident radiotracer accumulation was found in most of the CPs (86.7%). Interestingly, in as much as 29.1% of lesions with increased tracer uptake, concordant calcification was found in at least some part of the CP, possibly indicating that fatty acid synthesis may also be observed in CP. Another hypothesis for radiotracer accumulation in calcified lesions might be nonspecific tracer binding to arterial calcifications, as observed by Laitinen et al. for ^{18}F-FDG (*30*). However, it is currently not known whether—and to what extent—nonspecific mechanisms are involved in the vascular accumulation of tracers other than ^{18}F-FDG.

With regard to the intensity of ^{11}C-acetate accumulation in arterial lesions, the measured TBRs were comparable with those for other established tracers for plaque imaging. In a study by Rominger et al., mean TBR for vascular ^{18}F-FDG uptake in the abdominal aorta was 1.57 ± 0.35 (*11*). In another study using ^{18}F-sodium fluoride for visualization of mineral deposition in plaque, mean TBR was 2.3 ± 0.7 (*29*). In the present study, the mean intensity of tracer uptake as determined by TBR was 2.5 ± 1.0, underlining the excellent vascular contrast for ^{11}C-acetate, which facilitates evaluation of large arteries. The highest intensity of ^{11}C-acetate uptake was found in the abdominal aorta, which was true for both TBR and SUV_{max}. This is in line with previous studies using other tracers such as ^{18}F-FDG—studies that observed the highest TBRs in the aortic wall (*11*), although some have reported higher TBR values for the carotid arteries as compared with aortic territories (*31*). However, the intensity of arterial tracer uptake may be associated with plaque-specific factors including size or inflammatory state rather than with the localization of an artery within the arterial tree.

Both plaque composition and intraplaque distribution of biologic markers vary between intact and disrupted plaques. For instance, concentrations of fatty acids are increased at the edge of disrupted plaques, compared with the center (*5*). Interestingly, the extent of inflammation as determined by macrophage concentrations particularly at the plaque shoulders appears to correlate with degree of vulnerability (*32*). It would be highly desirable to obtain comparative data from the relative distribution of ^{18}F-FDG, ^{18}F-fluoride, and ^{11}C-acetate uptake within atheroma to assess the relative contribution of these tracers for the functional evaluation of different pathophysiologic processes in atherosclerotic plaque. Autoradiographic studies and histologic evaluation might lead to a better understanding of the involved mechanisms of intralesional tracer accumulation.

Fatty acid synthesis is an energy-consuming process creating fatty acids through action of the multifunctional enzyme FAS. First, ^{11}C-acetate is converted into ^{11}C-acetyl-CoA by acetyl-CoA synthetase inside the cell (*33*). Once ^{11}C-acetyl-CoA is formed, it may be used in de novo lipogenesis. After priming with acetyl-CoA, FAS synthesizes palmitate and other saturated fatty acids using malonyl-CoA as substrate, whereby the latter is formed by decarboxylating acetyl-coA (*19*). The main classes of lipids in atherosclerotic lesions—that is, cholesteryl esters, triglycerides, and phospholipids—all contain fatty acids (*16*). ^{11}C-acetate PET may be used to in vivo visualize the first biochemical reactions of fatty acid synthesis in plaque. On the one hand, these fatty acids are crucial for macrophage differentiation and

foam cell formation (*21*). On the other hand, fatty acids are involved in intralesional lipid homeostasis and macrophage inflammatory responses through action of peroxisome proliferator-activated receptors and liver X receptors (*3*). Therefore, ^{11}C-acetate depicts molecular processes in a manner different from ^{18}F-FDG or choline compounds, which may be used to provide information about macrophage-mediated inflammation or cell membrane proliferation in atherosclerotic lesions (*34,35*). The increasing number of tracers available for the characterization of pathophysiologic processes in atherosclerotic plaque—and their complementary use—may eventually lead to a more thorough understanding of the complex interactions in the development and evolution of plaque.

Recently, Schneider et al. demonstrated that FAS deficiency in macrophages decreases diet-induced atherosclerosis by inactivating FAS in macrophages of apolipoprotein E–deficient mice. In these knock-out mice, compared with wild-type mice, the extent of atherosclerosis was decreased 20%–40% in different aortic regions, underlining the crucial role of FAS in the development of atherosclerotic plaque (*22*). In another work, Ecker et al. demonstrated that induction of fatty acid synthesis is a key requirement for the development of phagocytic capacity in human monocytes and that suppression of fatty acid synthesis prevents uptake of lipoproteins such as enzymatically modified low-density lipoprotein (*21*). These findings demonstrate that inhibition of FAS might decrease foam cell development. Therefore, ^{11}C-acetate PET has the potential to provide new insights into the biology of fatty acid synthesis and macrophage differentiation in atherosclerotic plaque.

Fatty acid synthesis is dramatically increased in malignant cells (*36*). Because of the strong expression of FAS in these cells, considerable interest has been shown in the discovery and development of pharmacologic agents that block FAS activity, such as C75 or cerulenin (*36,37*). If suitable clinical FAS inhibitors become available, they may also prevent de novo fatty acid synthesis in atherosclerotic plaque (*22*). The incorporation of ^{11}C-acetate PET into preclinical models and clinical therapy monitoring studies could provide a promising technology to image fatty acid synthesis or the inhibition of FAS in plaque and could therefore represent a unique opportunity for in vivo target validation.

The present study had limitations. First, PET/CT was performed in oncologic patients, and therefore its findings might not be perfectly generalizable to other patient populations. However, factors that might influence tracer uptake in the arterial wall were carefully excluded. Second, a relatively small number of patients ($n = 36$) was included in this pilot study, influencing the statistical power to detect significant associations with atherogenic risk factors, because it has been shown that large patient cohorts are needed to reproduce known significant correlations in PET/CT of atherosclerotic plaque (*29*). However, such correlations have been observed in the present study for both age and sex, indicating an association of ^{11}C-acetate uptake with cardiovascular risk. Additionally, dynamic imaging might provide further information about the nature of tracer uptake in vessel wall alterations. Finally, as an intrinsic limitation of ^{11}C-acetate, assessment of relevant arteries such as the right coronary artery using ^{11}C-acetate is impaired because of high uptake of this tracer in the liver. Additionally, the clinical use of ^{11}C-acetate is limited by its short half-life, but synthesis of fluorinated ^{18}F-acetate is possible and might overcome that limitation (*23*). The results of this study need to be prospectively evaluated in a larger patient cohort to further explore the experimental and clinical potential of ^{11}C-acetate PET for imaging of fatty acid synthesis in arterial lesions, particularly for therapy-monitoring studies.

CONCLUSION

On the basis of in vitro findings of de novo fatty acid synthesis in atherosclerotic plaque, we demonstrated the feasibility of using ^{11}C-acetate PET/CT for imaging of arterial wall alterations. ^{11}C-acetate PET may allow for in vivo noninvasive quantification of fatty acid synthesis in the arterial wall. This study provides a rationale to incorporate ^{11}C-acetate PET into further preclinical and clinical studies to obtain new insights into fatty acid synthesis in atherosclerotic lesions and to evaluate whether it may be used to monitor pharmacologic intervention with FAS inhibitors.

DISCLOSURE STATEMENT

The costs of publication of this article were defrayed in part by the payment of page charges. Therefore, and solely to indicate this fact, this article is hereby marked "advertisement" in accordance with 18 USC section 1734.

ACKNOWLEDGMENT

No potential conflict of interest relevant to this article was reported.

REFERENCES

1. Lloyd-Jones D, Adams RJ, Brown TM, et al. Heart disease and stroke statistics: 2010 update—a report from the American Heart Association. *Circulation.* 2010;121:e46–e215.
2. Stewart ST, Cutler DM, Rosen AB. Forecasting the effects of obesity and smoking on U.S. life expectancy. *N Engl J Med.* 2009;361:2252–2260.
3. Chen W, Bural GG, Torigian DA, et al. Emerging role of FDG-PET/CT in assessing atherosclerosis in large arteries. *Eur J Nucl Med Mol Imaging.* 2009; 36:144–151.
4. Little WC, Constantinescu M, Applegate RJ, et al. Can coronary angiography predict the site of a subsequent myocardial infarction in patients with mild-to-moderate coronary artery disease? *Circulation.* 1988;78:1157–1166.
5. Felton CV, Crook D, Davies MJ, et al. Relation of plaque lipid composition and morphology to the stability of human aortic plaques. *Arterioscler Thromb Vasc Biol.* 1997;17:1337–1345.
6. Matter CM, Stuber M, Nahrendorf M. Imaging of the unstable plaque: how far have we got? *Eur Heart J.* 2009;30:2566–2574.
7. Tracy RE, Devaney K, Kissling G. Characteristics of the plaque under a coronary thrombus. *Virchows Arch A Pathol Anat Histopathol.* 1985;405:411–427.
8. Maseri A, Fuster V. Is there a vulnerable plaque? *Circulation.* 2003;107:2068–2071.
9. Trivedi RA, U-King-Im JM, Graves MJ, et al. MRI-derived measurements of fibrous-cap and lipid-core thickness: the potential for identifying vulnerable carotid plaques in vivo. *Neuroradiology.* 2004;46:738–743.

10. Perrone-Filardi P, Dellegrottaglie S, Rudd JH, et al. Molecular imaging of atherosclerosis in translational medicine. *Eur J Nucl Med Mol Imaging.* 2011;38:969–975.
11. Rominger A, Saam T, Wolpers S, et al. ^{18}F-FDG PET/CT identifies patients at risk for future vascular events in an otherwise asymptomatic cohort with neoplastic disease. *J Nucl Med.* 2009;50:1611–1620.
12. Rudd JH, Myers KS, Bansilal S, et al. Atherosclerosis inflammation imaging with ^{18}F-FDG PET: carotid, iliac, and femoral uptake reproducibility, quantification methods, and recommendations. *J Nucl Med.* 2008;49:871–878.
13. Rudd JH, Warburton EA, Fryer TD, et al. Imaging atherosclerotic plaque inflammation with [^{18}F]-fluorodeoxyglucose positron emission tomography. *Circulation.* 2002;105:2708–2711.
14. Kato K, Schober O, Ikeda M, et al. Evaluation and comparison of ^{11}C-choline uptake and calcification in aortic and common carotid arterial walls with combined PET/CT. *Eur J Nucl Med Mol Imaging.* 2009;36:1622–1628.
15. Derlin T, Richter U, Bannas P, et al. Feasibility of ^{18}F-sodium fluoride PET/CT for imaging of atherosclerotic plaque. *J Nucl Med.* 2010;51:862–865.
16. Insull W Jr, Bartsch GE. Cholesterol, triglyceride, and phospholipid content of intima, media, and atherosclerotic fatty streak in human thoracic aorta. *J Clin Invest.* 1966;45:513–523.
17. Filipovic I, Rutemoller M. Comparative studies on fatty acid synthesis in atherosclerotic and hypoxic human aorta. *Atherosclerosis.* 1976;24:457–469.
18. Whereat AF. Lipid biosynthesis in aortic intima from normal and cholesterol-fed rabbits. *J Atheroscler Res.* 1964;4:272–282.
19. Semenkovich CF. Regulation of fatty acid synthase (FAS). *Prog Lipid Res.* 1997;36:43–53.
20. Glass CK, Witztum JL. Atherosclerosis: the road ahead. *Cell.* 2001;104:503–516.
21. Ecker J, Liebisch G, Englmaier M, et al. Induction of fatty acid synthesis is a key requirement for phagocytic differentiation of human monocytes. *Proc Natl Acad Sci USA.* 2010;107:7817–7822.
22. Schneider JG, Yang Z, Chakravarthy MV, et al. Macrophage fatty-acid synthase deficiency decreases diet-induced atherosclerosis. *J Biol Chem.* 2010;285:23398–23409.
23. Jadvar H. Prostate cancer: PET with ^{18}F-FDG, ^{18}F- or ^{11}C-acetate, and ^{18}F- or ^{11}C-choline. *J Nucl Med.* 2011;52:81–89.
24. Herrero P, Kim J, Sharp TL, et al. Assessment of myocardial blood flow using ^{15}O-water and 1-^{11}C-acetate in rats with small-animal PET. *J Nucl Med.* 2006;47:477–485.
25. Jambor I, Borra R, Kemppainen J, et al. Functional imaging of localized prostate cancer aggressiveness using ^{11}C-acetate PET/CT and ^{1}H-MR spectroscopy. *J Nucl Med.* 2010;51:1676–1683.
26. Tahara N, Kai H, Ishibashi M, et al. Simvastatin attenuates plaque inflammation: evaluation by fluorodeoxyglucose positron emission tomography. *J Am Coll Cardiol.* 2006;48:1825–1831.
27. Dunphy MP, Freiman A, Larson SM, et al. Association of vascular ^{18}F-FDG uptake with vascular calcification. *J Nucl Med.* 2005;46:1278–1284.
28. Ben-Haim S, Kupzov E, Tamir A, et al. Evaluation of ^{18}F-FDG uptake and arterial wall calcifications using ^{18}F-FDG PET/CT. *J Nucl Med.* 2004;45:1816–1821.
29. Derlin T, Toth Z, Papp L, et al. Correlation of inflammation assessed by ^{18}F-FDG PET, active mineral deposition assessed by ^{18}F-Fluoride PET, and vascular calcification in atherosclerotic plaque: a dual-tracer PET/CT study. *J Nucl Med.* 2011;52:1020–1027.
30. Laitinen I, Marjamäki P, Haaparanta M, et al. Non-specific binding of [^{18}F]FDG to calcifications in atherosclerotic plaques: experimental study of mouse and human arteries. *Eur J Nucl Med Mol Imaging.* 2006;33:1461–1467.
31. Rudd JH, Myers KS, Bansilal S, et al. ^{18}Fluorodeoxyglucose positron emission tomography imaging of atherosclerotic plaque inflammation is highly reproducible: implications for atherosclerosis therapy trials. *J Am Coll Cardiol.* 2007;50:892–896.
32. Zheng J, El Naqa I, Rowold FE, et al. Quantitative assessment of coronary artery plaque vulnerability by high-resolution magnetic resonance imaging and computational biomechanics: a pilot study ex vivo. *Magn Reson Med.* 2005;54:1360–1368.
33. Ikeda Y, Yamamoto J, Okamura M, et al. Transcriptional regulation of the murine acetyl-CoA synthetase 1 gene through multiple clustered binding sites for sterol regulatory element-binding proteins and a single neighboring site for Sp1. *J Biol Chem.* 2001;276:34259–34269.
34. Saam T, Rominger A, Wolpers S, et al. Association of inflammation of the left anterior descending coronary artery with cardiovascular risk factors, plaque burden and pericardial fat volume: a PET/CT study. *Eur J Nucl Med Mol Imaging.* 2010;37:1203–1212.
35. Yoshimoto M, Waki A, Obata A, et al. Radiolabeled choline as a proliferation marker: comparison with radiolabeled acetate. *Nucl Med Biol.* 2004;31:859–865.
36. Kuhajda FP, Pizer ES, Li JN, et al. Synthesis and antitumor activity of an inhibitor of fatty acid synthase. *Proc Natl Acad Sci USA.* 2000;97:3450–3454.
37. Kridel SJ, Lowther WT, Pemble CW. Fatty acid synthase inhibitors: new directions for oncology. *Expert Opin Investig Drugs.* 2007;16:1817–1829.